JOURNAL OF APPLIED ELECTROCHEMISTRY **18** (1988) 142–148

Polarization of lead-tin alloys in sulphuric acid

M. N. C. IJOMAH

Department of Metallurgy & Materials Engineering, Anambra State University of Technology, PMB 01660, Enugu, Nigeria

Received 9 May 1987; revised 1 September 1987

The electrochemical behaviour of a series of Pb-Sn alloys in 30% sulphuric acid has been studied. Potentiodynamic current transients were recorded for the respective alloys, in the potential range between hydrogen and oxygen evolution. These were carefully studied and subsequently correlated with electrochemical, complex plane impedance data. The results obtained were used to isolate the electrode processes prevailing at the various potentials and to determine the nature of the protective films formed, thus elucidating the mechanism of passivation. Implications in corrosion behaviour are discussed.

1. Introduction

The electrochemical behaviour of lead in sulphuric acid has been extensively studied [1–9, 11, 13–17]. When lead is polarized in sulphuric acid in the potential range between hydrogen and oxygen evolution, typifying the active, passive and trans-passive regions, a number of reactions occur, two of which represent the charge and discharge reactions of the lead-acid battery, namely:

$$\text{(a) } Pb + SO_4^{2-} \underset{c}{\overset{d}{\rightleftharpoons}} PbSO_4 + 2e \quad (1)$$

$$\text{(b) } PbO_2 + SO_4^{2-} + 4H^+ + 2e \underset{c}{\overset{d}{\rightleftharpoons}} PbSO_4 + 2H_2O \quad (2)$$

The passivity of lead in sulphuric acid apparently follows the appearance of the virtually insoluble and non-conducting $PbSO_4$ film on the specimen surface, a phenomenon which is yet to be fully understood. The present work, although very much at the exploratory stage, seeks to compare the potential versus current behaviour of some binary Pb-Sn alloys with their electrochemical impedance spectra. The impedance concept assumes that a corroding electrode exhibits an intricate electrochemical behaviour which depends on several factors, namely: the ionic and electronic resistance of the solution and the bulk of the electrode film; the double layer capacitance resulting from interfacial build-up of water dipoles, adsorbed ions and organic molecules; a charge transfer resistance arising from the anodic and cathodic electrochemical reactions; the relative effects of diffusion (Warburg factor) and that of reactant and product adsorption on the electrode surface. The overall response has been hypothetically represented by a network of circuit elements, comprising resistance, inductance and capacitance, similar in behaviour to the corroding electrode [18–35]. The purpose of this work is to identify the dominant electrode processes either favouring or hindering passivity, to elucidate the mechanism of passivation and describe corrosion behaviour.

2. Experimental details

2.1. *Specimen preparation*

Pure Pb was melted in a silica-graphite crucible, under an argon atmosphere. Pure Sn granules were then added to the melt and the mixture was heated to 350° C. Adequate mixing was ensured by stirring the melt rapidly and letting it stand for a few minutes before pouring into a pre-heated (200° C) steel mould, to give a cylindrical specimen. The composition of the alloy was varied by controlling the amounts of Sn and extra Pb added to the melt. All alloying additions were of Analar grade. A test sample was cut from each alloy and electrical connection was provided by soldering a Cu wire to one end of the specimen. The soldered joint and sides of the specimen were later sealed off with 'Araldite' adhesive to expose a circular area of 0.224 cm^2.

2.2. *Potentiodynamic current measurements*

The lead alloy specimen was polished using SiC papers. While still wet from the final polishing, the specimen was introduced into the cell and connected to the appropriate terminal of a 'Wenking' 70TS1 potentiostat to which a linear sweep unit was linked. The linear sweep unit allowed the potential of the working electrode (specimen) to vary uniformly at a pre-determined rate, within a potential range established by two set limits. A rest (open circuit) potential of about −1100 mV was registered by the freshly polished specimen, but this gradually dropped and tended to stabilize at about −950 mV after about 3 min immersion. Both anodic and cathodic sweeps were carried out. An X–Y chart recorder was used to monitor the potential versus current behaviour while a digital voltmeter connected across the working electrode and the reference displayed the corresponding electrode potential. A 3-electrode cell was used for all polarization measurements. The counter electrode was a 2 cm × 1.5 cm platinum foil welded to a

0021-891X/88 $03.00 + .12

platinum wire. A mercury-mercurous sulphate electrode (690 mV versus SHE) was employed as reference. A sweep speed of 180 mV per minute was generally used.

2.3. *Electrode impedance measurements*

The freshly polished specimen was introduced into the cell and left to stand for about 10 min prior to the test. Impedance measurements were carried out using an automated transfer function analyser which basically consisted of a 'Solartron' 1172 frequency response analyser and a data transfer unit. A downward frequency sweep, from 10 kHz to 0.1 mHz, was carried out with a sinusoidal a.c. input signal of 10 mV (r.m.s.) amplitude superimposed on the constant d.c. voltage applied to the working electrode. The resultant current and voltage outputs were correlated and the result displayed in the form of complex variables (a, b) and subsequently analysed by computer. A fresh specimen surface was used for each impedance measurement.

Table 1. Standard redox reactions of the lead electrode in sulphuric acid and the corresponding electrode potentials [13, 15, 36]

Electrode reactions	*Potential,* E_0 (mV) (vs SHE)	vs Hg/Hg_2SO_4
$PbSO_4 + 2e = Pb + SO_4^{2-}$	(−360)	−1050
$Sn = Sn^{2+} + 2e$	(−140)	−830
$PbO \cdot PbSO_4 + 2H^+ + 4e = 2Pb + SO_4^{2-} + H_2O$	(−110)	−800
$Sn^{2+} = Sn^{4+} + 2e$	(150)	−540
$PbO + 2H^+ + 2e = Pb + H_2O$	(250)	−440
$PbO_2 + 2H^+ + 2e = PbO + H_2O$	(1110)	420
$2PbO_2 + SO_4^{2-} + 6H^+ + 4e = PbO \cdot PbSO_4 + 3H_2O$	(1470)	780
$PbO_2 + 4H^+ + 2e = Pb^{2+} + 2H_2O$	(1480)	790
$PbO_2 + 4H^+ + SO_4^{2-} + 2e = PbSO_4 + 2H_2O$	(1690)	1000

3. Results

3.1. *Potential-current behaviour*

The potentiodynamic (linear sweep) curves for the pure Pb and pure Sn specimen are shown in Fig. 1. For the pure Pb specimen, a peak current was recorded at about −1050 mV, corresponding to the formation of $PbSO_4$ according to the scheme: $Pb + SO_4^{2-} = PbSO_4 + 2e$ (see Table 1). Following this peak, the current dropped to a very low value indicative of the attainment of passivity and maintained this residual threshold value for a considerable potential range (passive region) before rising steeply with oxygen evolution (trans-passivity). For the pure Sn specimen, only secondary passivity was conferred following the $SnSO_4$ peak. The current rose to a high value and subsequently climbed through a shallow peak (hump) before rising very steeply. The potential versus current behaviour for the dilute Pb-Sn alloys (Fig. 2) essentially followed the characteristic behaviour of the pure Pb specimen, portraying the $PbSO_4$ peak at about −1050 mV, followed by the low residual current (passivity) and finally the steep current rise at elevated potentials (E > 1500 mV). No definite peak was recorded for PbO_2. It was believed that conversion of $PbSO_4$ to PbO_2 occurred simultaneously with oxygen evolution. A cathodic (reverse) sweep was then carried

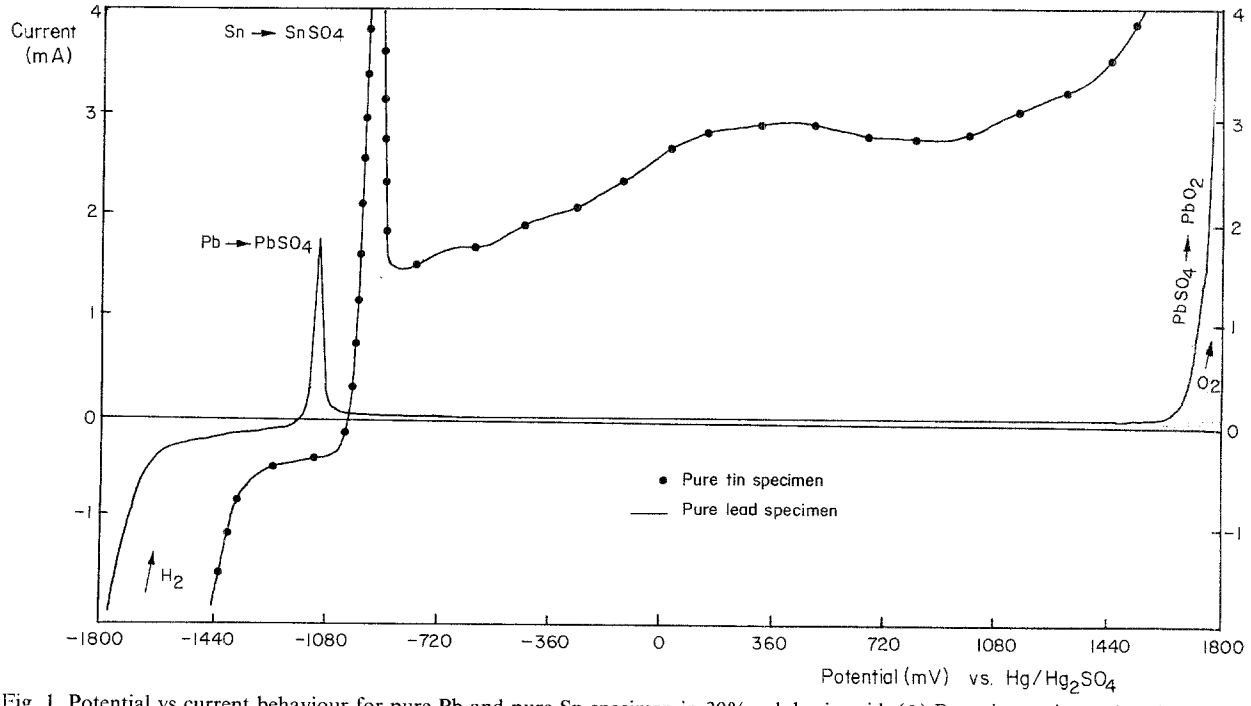

Fig. 1. Potential vs current behaviour for pure Pb and pure Sn specimen in 30% sulphuric acid. (●) Pure tin specimen; (——) pure lead specimen.

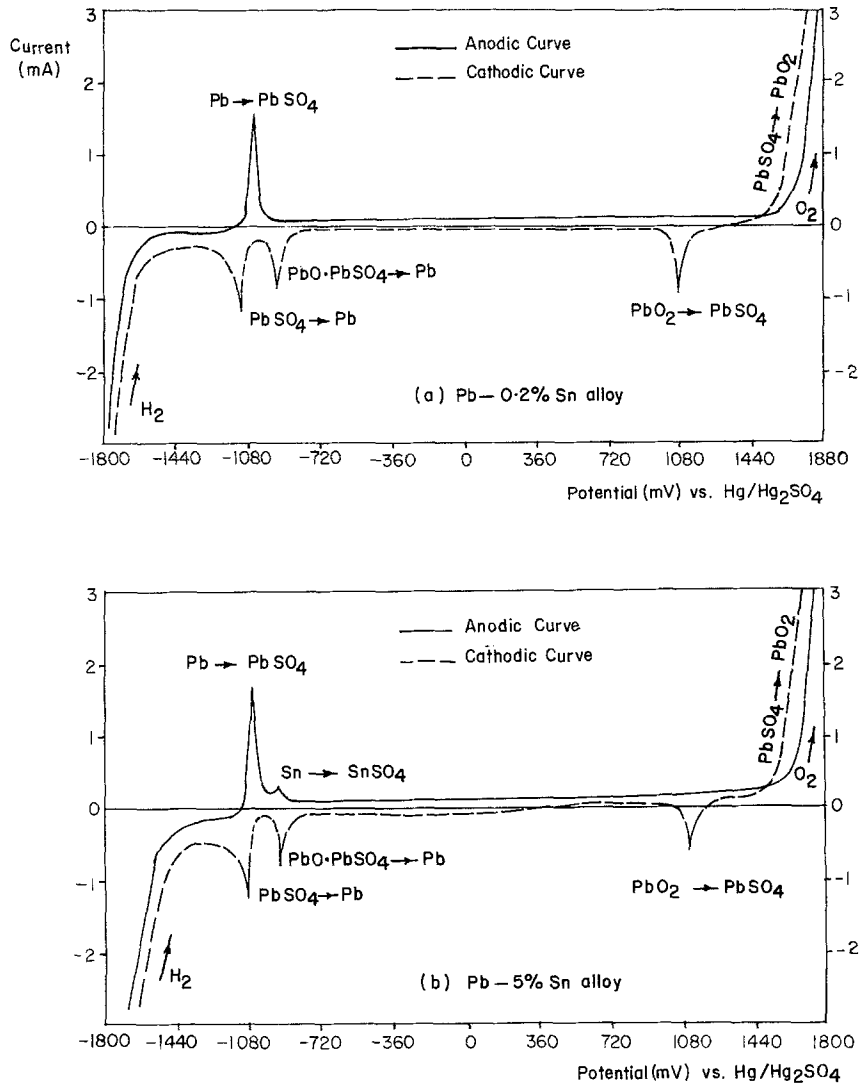

Fig. 2. Potential versus current behaviour for the dilute Pb-Sn alloys in 30% sulphuric acid. (——) Anodic curve; (– – –) cathodic curve.

out in order to confirm the various compounds earlier formed on the specimen and to identify any peaks that might be missed during the anodic sweep. A reduction peak, apparently PbO_4 to $PbSO_4$, was recorded at about 1080 mV, thereby supporting the earlier view that the compound formed during oxygen evolution, while the peaks at −800 mV and −1100 mV respectively corresponded to the reduction of $PbO \cdot PbSO_4$ and $PbSO_4$ to metallic Pb. For the Pb-5%Sn alloy (Fig. 2b), a current shoulder was recorded at −850 mV which apparently represented the conversion of Sn to $SnSO_4$, although the corresponding $SnSO_4$ peak was not observed during the cathodic sweep. The potential versus current behaviour for the concentrated Pb-Sn alloys (Fig. 3) was essentially characterized by the $PbSO_4$ oxidation peak, the well defined $SnSO_4$ peak and a multiple hump (−360 mV to 720 mV) preceding the steep rise towards transpassivity. On the reverse sweep, the $SnSO_4$ reduction peak (−900 mV) was distinctly observed, between the $PbSO_4$ and $PbO \cdot PbSO_4$ reduction peaks. However, the PbO_2 reduction peak was not observed in the Pb-60%Sn alloy specimen (Fig. 3b), an indication that the resultant film contained very little PbO_2, but rather consisted essentially of $PbSO_4$, $SnSO_4$ and possibly soluble SnO and SnO_2 which subsequently went into solution, leaving a highly porous film, hence the high anodic current recorded.

3.2. *Influence of sweep speed*

The effect of changing sweep speed on the polarization curves is shown on Fig. 4. During the potentiodynamic tests, electroactive species were progressively removed in the vicinity of the electrode, somehow causing a current limitation. The anodic reaction, $Pb + SO_4^{2-} = PbSO_4 + 2e$, was apparently limited by the depletion of SO_4^{2-} ions in the neighbourhood of the electrode. A slow sweep speed increased this limitation, thereby reducing the height of the peak (Fig. 4a), while a fast sweep decreased the current limitation, thus increasing the magnitude of the peak (Fig. 4b). The cathodic peaks (reduction reactions), on the other hand, were apparently limited by diffusion through the external film. Consequently, a fast sweep (Fig. 4b) tended to increase this limitation and reduced the magnitude of the cathodic peaks, while a slow sweep (Fig. 4a), had the opposite effect. Furthermore, a fast sweep speed tended to widen the passive region, a phenomenon not yet fully investigated, but certainly not unconnected with the suppression of oxygen evolution, a reaction which involves specific

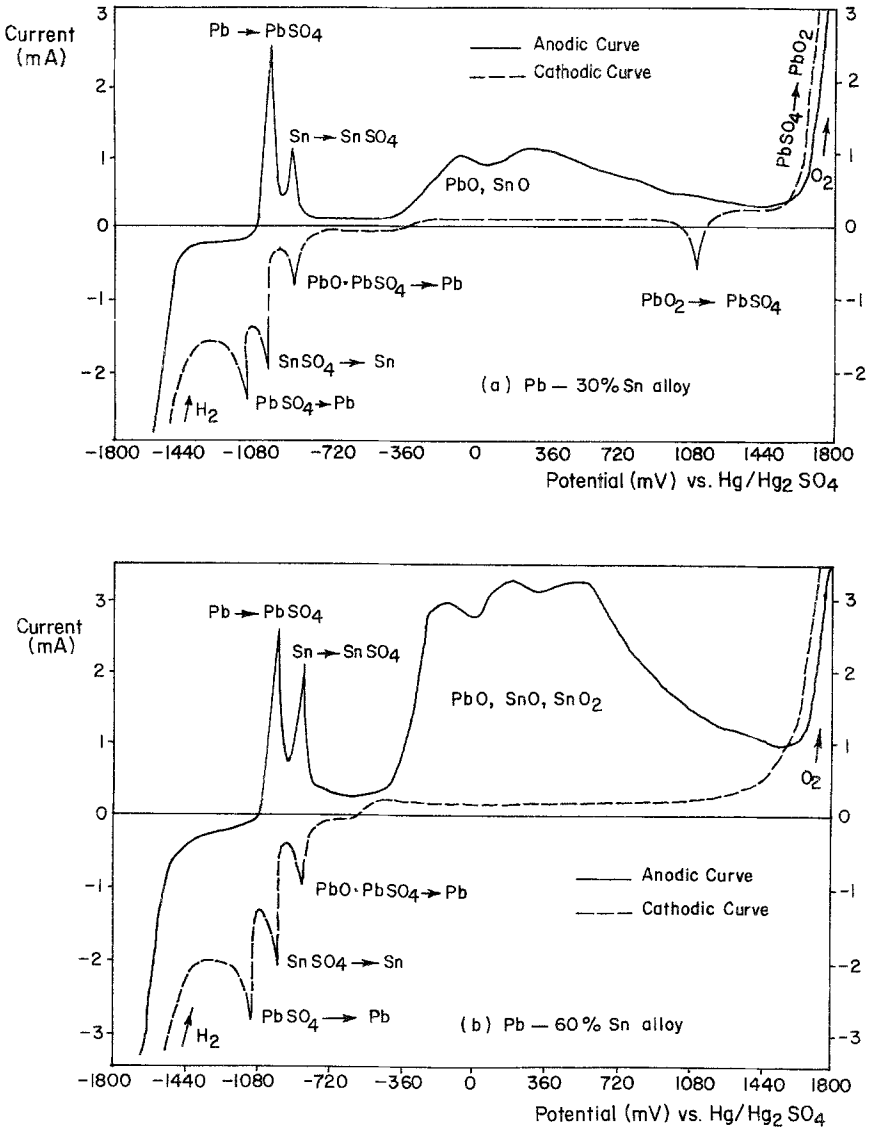

Fig. 3. Potential versus current behaviour for the concentrated Pb-Sn alloys in 30% sulphuric acid. (——) Anodic curve; (– – –) cathodic curve.

site adsorption of oxygen, surface conversion of $PbSO_4$ and desorption of oxygen molecules, which are time dependent.

3.3. *Electrochemical impedance spectra*

The impedance measurements for the Pb-0.2%Sn alloy specimen in the active, passive and trans-passive regions are summarized in Figs 5, 6 and 7. The impedance plot at -1100 mV (Fig. 5) was characterized by a full charge transfer resistance semicircle indicative of a purely activation controlled process, i.e. active metal dissolution in accordance with the scheme: $Pb = Pb^{2+} + 2e$, with an estimated charge transfer resistance (R_θ) of 250 Ω cm^2. At a potential of -1000 mV, a smaller charge transfer resistance semicircle ($R_\theta = 95\,\Omega\,cm^2$) was recorded which appeared distorted at lower frequencies to form a straight line (Warburg effect) indicative of enhanced metal dissolution ($PbSO_4$ current peak), under diffusion control. Apparently, the process was limited by diffusion of SO_4^{2-} towards the electrode or conversely, the diffusion of dissolved species (Pb^{2+}) away from the electrode. At about -900 mV, the impedance plot was virtually a straight line indicating pure diffusion control ($R_\theta = \infty$). Here, $PbSO_4$ was believed to have precipitated on the electrode surface, apparently at a critical surface super-saturation of dissolving Pb^{2+} ions, and exerting a purely capacitive effect, i.e. for subsequent reaction to occur, ions must be conducted through this layer. This signifies the onset of passivity, a phenomenon previously emphasized by the potentiodynamic curve (Fig. 2a), the low residual current indicating the rate of ionic transport through the pores of the $PbSO_4$ film. Similar impedance spectra were recorded at -700 mV and -500 mV respectively, showing that the $PbSO_4$ film still offered maximum resistance to charge transfer. It was previously noted that the potential versus current behaviour was typically flat over this region. The impedance plot at 200 mV (Fig. 6) again portrayed the characteristic charge transfer resistance semicircle, albeit limited by diffusion. Intermediate compounds PbO, SnO, etc., were believed to form beneath the $PbSO_4$ film at about this potential and the process was limited by diffusion through the external film. It was noted that the passive current started fluctuating at about this potential during the potentiodynamic sweep, with the level of disturbance, or instability, increasing with alloying concentration (see Figs 2 and 3). A similar impedance

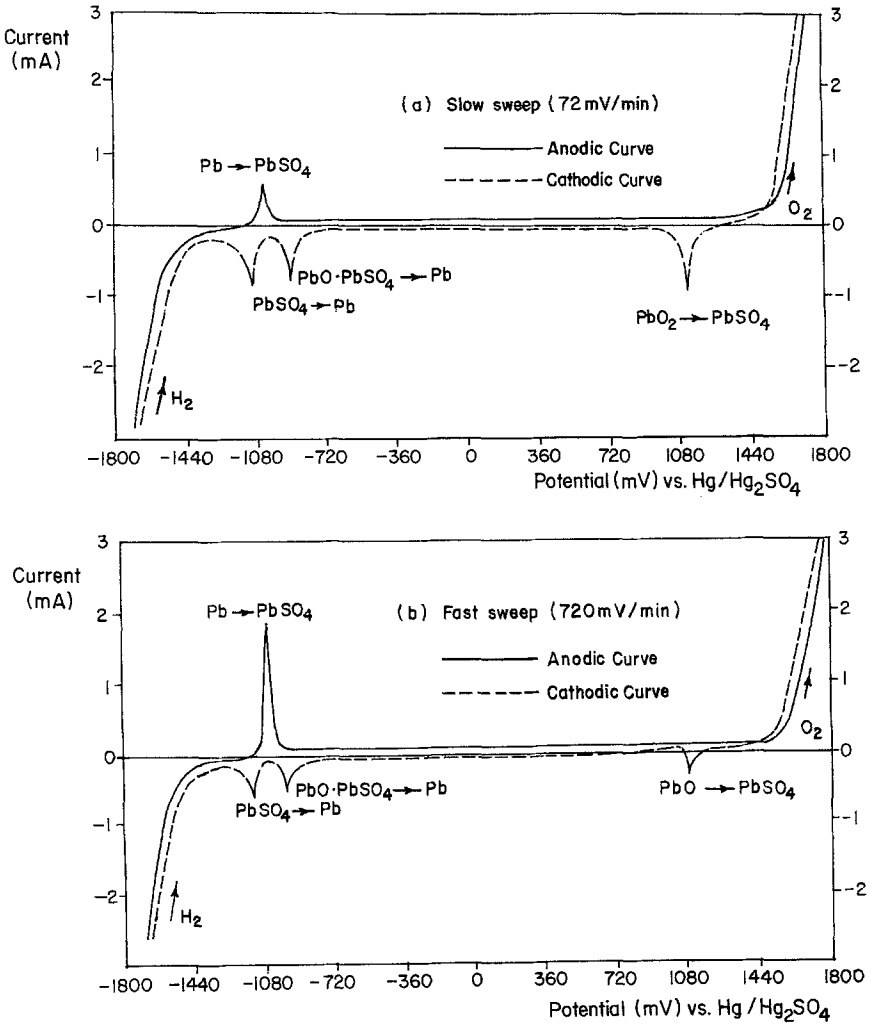

Fig. 4. Effect of changing sweep speed on polarization behaviour. (——) Anodic curve; (– – –) cathodic curve.

plot was recorded at 700 mV and 900 mV with increasing Warburg effect or diffusion control, an obvious indication of film thickening. The impedance spectra recorded at 1000 mV, 1100 mV and 1200 mV (Fig. 7) were intricate plots. PbO_2 was believed to form within this range, the mechanism of which apparently involved a number of processes including the adsorption of oxygen at the electrode surface and its subsequent desorption (oxygen evolution), partial dissolution (surface conversion) of the $PbSO_4$ film and the inward

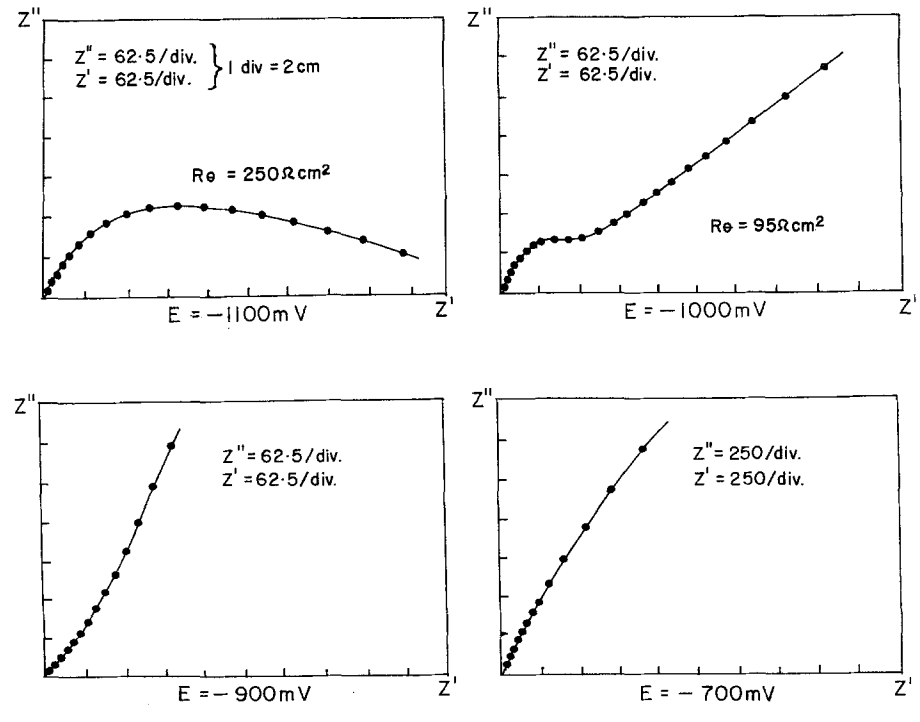

Fig. 5. Complex plane impedance spectra for the Pb-0.2%Sn specimen in 30% sulphuric acid, from −1100 mV to −700 mV ($Z = Z' + jZ''$).

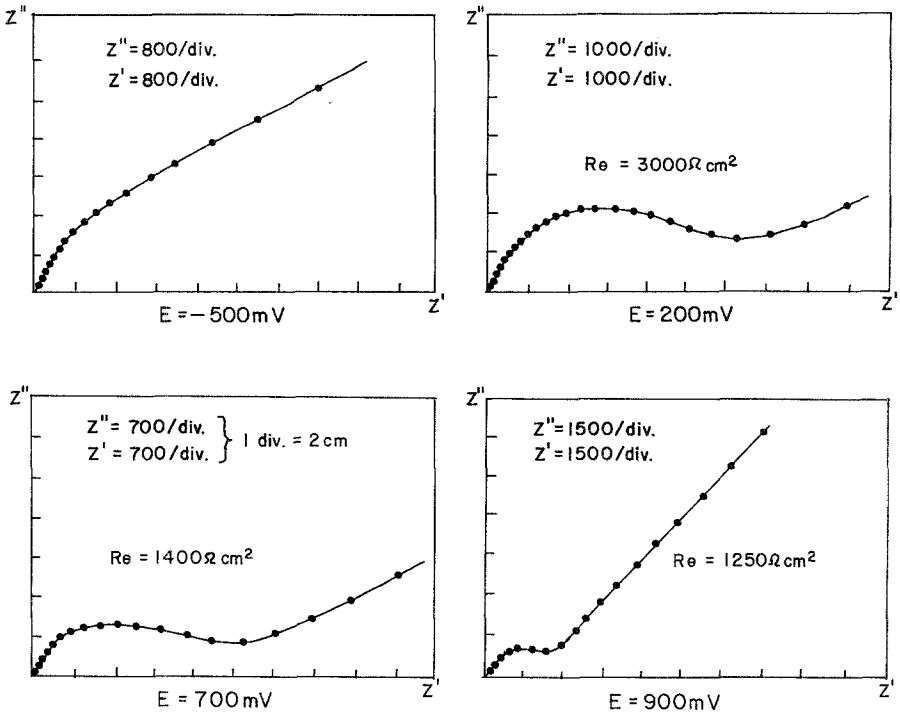

Fig. 6. Complex plane impedance spectra for the Pb-0.2%Sn specimen in 30% sulphuric acid, from −500 mV to 900 mV ($Z = Z' + jZ''$).

growth of the PbO_2 film, a reaction limited by diffusion through the surface film. Finally, the impedance plot at about 1500 mV showed a charge transfer resistance semicircle depressed into a pear-like shape by the effects of adsorption. Metal dissolution was thought to become significant at this potential, with obvious implication in lead-acid battery technology (overcharge corrosion). The intense oxygen evolution at the specimen surface apparently involved an adsorption stage.

4. Discussion

In this exploratory work, a series of Pb-Sn alloys were polarized in 30% sulphuric acid (pH = −0.6) in the potential range typifying the active, passive and transpassive regions, i.e. −1100 mV to 1500 mV, versus the mercury-mercurous sulphate reference. A number of important findings were made and there is good agreement between the potential versus current behaviour and the resultant impedance measurements. The passivity of Pb-Sn alloys in sulphuric acid, depends primarily upon the presence of a virtually insoluble $PbSO_4$ film at the specimen surface, apparently at a critical surface super-saturation of dissolving Pb^{2+} ions, a process which involves a solution precipitation mechanism as well as three-dimensional growth [6, 8, 16, 17, 30]. The $PbSO_4$ film is believed to be of duplex structure, comprising a $PbSO_4$ matrix and $PbO \cdot PbSO_4$ at the intercrystalline spaces where local alkalinity

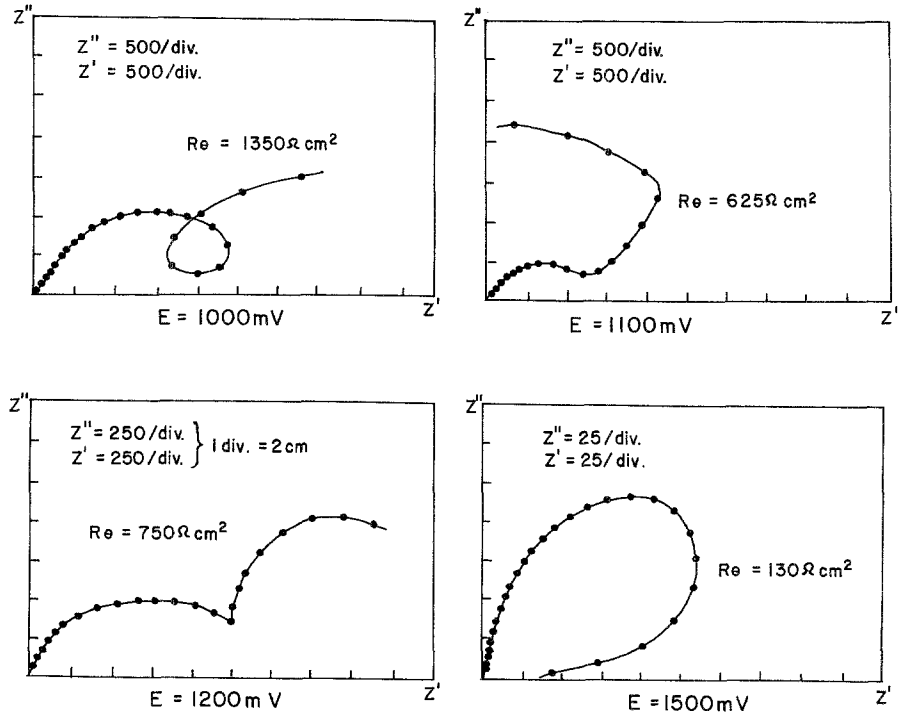

Fig. 7. Complex plane impedance spectra for the Pb-0.2%Sn specimen in 30% sulphuric acid, from 1000 mV to 1500 mV ($Z = Z' + jZ''$).

is enhanced. Hence, separate reduction peaks were recorded for $PbO \cdot PbSO_4$ and $PbSO_4$ during the potentiodynamic test. The presence of intermediate compounds was also confirmed during the test, albeit with some displacement in their respective electrode potentials compared with the predicted values (Table 1), which was not unexpected, considering ohmic polarization through the external film as well as the strong pH dependency of the various compounds, for example; PbO, SnO, PbO_2 and SnO_2 have a slope of 0.0591 vs pH [36]. Apparently, for the same reason, oxygen evolution occurred at a much higher potential in the 30% sulphuric acid. Oxidation of $PbSO_4$ to PbO_2 is believed to occur simultaneously with oxygen evolution, though the presence of a polymorphic film (α-PbO_2 and β-PbO_2) according to other workers [1–9, 16] could not be ascertained. A single reduction peak, PbO_2 to $PbSO_4$, was subsequently recorded, though the possibility of peaks overlapping could not be entirely discounted. The electrochemical behaviour of the concentrated Pb-Sn alloys is of particular significance. During the potentiodynamic sweep, the anodic current was generally high, with an irregular loop preceding oxygen evolution. It is believed that, in addition to PbO, sparingly soluble intermediate compounds, SnO and SnO_2, are also formed. For the Pb-60%Sn specimen, the PbO_2 cathodic peak was not observed and it was suggested that dissolution of SnO and SnO_2 competed with oxygen evolution, thus hindering the $PbSO_4$ to PbO_2 conversion process. Apparently, the resultant film contained very little PbO_2. Earlier work, using electron probe micro-analysis, confirmed the presence of Sn in the anodic film, even for dilute Pb-Sn alloys [17]. Thus, from current findings, it is evident that Sn is essentially incorporated as $SnSO_4$. The effect of changing sweep speed on polarization behaviour also helped to elucidate the mechanism of passivation. The impedance measurements obviously emphasized the conjoint effect of the electrode processes prevailing at any given potential, the charge transfer resistance of which ultimately determined corrosion rate, according to the well known Stern & Geary relation [37]:

$$i_{corr} = \frac{\beta_a \beta_c}{2.3 R_\theta (\beta_a + \beta_c)} = \frac{\text{constant}}{R_\theta} \qquad (3)$$

(where β_a and β_c are the anodic and cathodic Tafel slopes and R_θ is the charge transfer resistance analogous to the polarization resistance, R_p).

Generally, there was a strong correlation between potentiodynamic current behaviour and impedance data, except in the trans-passive region where intricate impedance plots were encountered. The above results were fairly reproducible and the general shape and trend was always maintained. However, slight differences did exist between successive polishing of individual specimens. This is not unconnected with the magnitude of surface roughness, i.e. polishing efficiency. The rougher the specimen surface, the greater the exposed surface area compared with the smoother surface, hence, the higher the magnitude of the current, although the current density remained essentially constant. A more detailed investigation is, however, required in the trans-passive region in order to fully isolate the processes involved in PbO_2 film growth. It may also be necessary to evaluate the polarization behaviour of an electropolished specimen.

References

[1] J. Lander, *J. Electrochem. Soc.* **98** (1951) 220.
[2] *Idem, ibid.* **103** (1956) 1.
[3] *Idem, ibid.* **98** (1951) 213.
[4] *Idem, ibid.* **99** (1952) 467.
[5] J. Burbank, *J. Electrochem. Soc.* **103** (1956) 87.
[6] *Idem, ibid.* **104** (1957) 693.
[7] *Idem, ibid.* **106** (1959) 369.
[8] P. Ruetschi and R. T. Angstadt, *J. Electrochem. Soc.* **111** (1964) 1323.
[9] J. Burbank, A. C. Simon and E. Willignganz, *Advances in Electrochemistry & Electrochemical Engineering* **8** (1971).
[10] W. Hofmann, 'Lead & Lead Alloys', Springer-Verlag, Berlin (1970).
[11] A. Marshall, R. Piercy and N. A. Hampson, *Corrosion Science* **15** (1975) 23.
[12] M. N. C. Ijomah, *Crystal Properties and Preparation* **9** (1986) 55.
[13] P. Delahay, M. Pourbaix and P. Van Rysselberghe, *J. Electrochem. Soc.* **98**, (1951) 57.
[14] G. W. Vinal, 'Storage Batteries', Wiley Press, N.Y. (1956).
[15] J. P. Carr and N. A. Hampson, *Chem. Reviews* **72** (1972) 679.
[16] D. Pavlov and N. Iordanov, *J. Electrochem. Soc.* **117** (1970) 1103.
[17] M. N. C. Ijomah, *ibid.* (to be published).
[18] J. E. B. Randles, *Discussions Faraday Soc.* **1** (1947) 11.
[19] H. Ershler, *ibid.* **1** (1947) 269.
[20] H. Gerischer, *Z. Physik. Chem.* **198** (1951) 286.
[21] D. C. Grahame, *J. Electrochem. Soc.* **99** (1952) 370c.
[22] H. Gerischer, *Z. Physik. Chem.* **202** (1953) 302.
[23] H. J. Vetter, *ibid.* **199** (1985) 285.
[24] R. H. Cole, *J. Chem. Phys.* **23** (1955) 493.
[25] J. Euler and K. Dehmelt, *Z. Electrochem.* **1** (1957) 1200.
[26] J. H. Sluyters, *Rec. Trav. Chim.* **79** (1960) 1092.
[27] *Idem, ibid.* **82** (1963) 100.
[28] M. Sluyters-Rehback and J. H. Sluyters, *Electroanal. Chem.* **4** (1969) 1.
[29] I. Epelboin and M. Keddam, *J. Electrochem. Soc.* **117** (1970) 1052.
[30] L. M. Baugh, K. L. Bladen and F. L. Tye, *J. Electroanal. Chem.* **145** (1983) 355.
[31] I. Epelboin, M. Keddam and H. Takenouti, *Z. Physic. Chem.* **98** (1975) 215.
[32] R. D. Armstrong and M. Handerson, *J. Electrochem. Chem.* **39** (1972) 81.
[33] R. D. Armstrong and K. Edmondson, *Electrochimica Acta* **18** (1973) 937.
[34] I. Epelboin, M. Keddam and H. Takenouti, *J. Appl. Electrochem.* **2** (1972) 71.
[35] G. Archdale and J. A. Harrison, *J. Electroanal. Chem.* **39** (1972) 357.
[36] M. Pourbaix, 'Atlas of Electrochemical Equilibria in Aqueous Solutions', Pergamon Press, N.Y. (1966).
[37] L. M. Callow, J. A. Richardson and J. L. Dawson, *British Corrosion Journal* **11** (1976) 123.